

# The Influence of Mg and Cr Addition on the Anodizing and Electrochemical Behaviors of 5xxx Al Alloy

C. I. CHANG\*, T. Y. TSENG\*, J. P. CHANG\*\*, J.S. GUO\*\* and C.K. KAO\*\*\*

\*New Materials Research & Development Department, China Steel Corporation

\*\* Research & Development Department, China Steel Aluminum Corporation

\*\*\* Rolling Mill I Department, China Steel Aluminum Corporation

The influence of Mg and Cr content on color of anodized films on 5xxx Al alloys was analyzed. Furthermore, measurements of potentiodynamic polarization curves (PDS), electrochemical impedance spectroscopy (EIS) and scanning electron microscopy (SEM) were utilized to investigate the effects of Mg and Cr addition on the corrosion and electrochemical behavior of 5xxx Al alloy in H<sub>2</sub>SO<sub>4</sub> or NaCl aqueous solution. The results of the anodizing treatment showed that with Cr addition, the color space b\*-value of anodized film increases and the color of the film becomes yellower. However, the b\*-value of anodized film decreased with increasing Mg content. The results of electrochemical tests showed that 5xxx Al alloy was more susceptible to corrosion with Mg addition due to a decrease of corrosion potential and impedance, and more resistant to corrosion with Cr addition. During the corrosion process, the initial corrosion attack took place on interfaces with a potential drop, such as interfaces between matrix and Mg-Si or Al-Fe particles. In the chloride solution, the increase of chloride concentration promotes the formation and propagation of pitting, and thus the corrosion resistance of 5xxx Al alloy dropped.

**Keywords:** 5xxx Al Alloy, Anodic Oxidation, Mg ∨ Cr Addition, Corrosion Behavior, Polarization Curve

## 1. INTRODUCTION

Aluminum alloy has advantages of light weight, high specific strength, good electrical conductivity, good corrosion resistance and formability. It is widely used in aerospace, 3C/IT and transportation industries. Among them, 5xxx (Al-Mg) Al alloy is widely used in the applications of 3C/IT products, such as notebooks, tablets, mobile phones and wearable products<sup>(1-2)</sup>. These 3C wearable products are required to be ultra-lightweight and have high surface quality. Hence, anodizing treatment is usually conducted in 5xxx Al alloys for the purposes of good wear resistance and decorative properties. In the pursuit of beauty in decorative surfaces with smaller size of 3C/IT products, how to improve mechanical strength of the Al sheet with good anodized surface quality is the main trend today.

Practically, alloying elements are usually added in aluminum alloys to adjust metallurgical or mechanical properties in order to meet the application requirements. In general, the 5xxx Al alloy can significantly increase the mechanical strength by adding Mg. For example, the YS and TS can be increased by as much as 18% and 26%, respectively, by adding Mg from 2wt% to 4wt% in 5xxx Al alloy. Besides the strength, the shades of the

anodic oxide film were also affected by the alloying element addition<sup>(3-6)</sup>. Tanaka et al.<sup>(7)</sup> found that the color space L\* value of anodic oxide film decreases with Si addition, and causes the color of the film to become darker. Ohnishi et al.<sup>(8)</sup> and Ishikawa et al.<sup>(9)</sup> also indicated that alloying elements such as Mg, Fe, Si, Mn affect the colors of the anodic oxide film. Among them, the CIE(L\*, a\*, b\*) color space L\* value and b\* value of the oxide film decreased with increasing Fe content, and the color tone of the film changed to brown. With element addition, electrochemical properties of Al alloys were also changed. Vrsalovic<sup>(10)</sup> found that the susceptibility towards localized type of corrosion is higher for Al alloy with 2.5wt%Mg than Al alloy with 0.8wt% Mg in 3.5wt% NaCl solution. Alternatively, Baldwin<sup>(11)</sup> found that by increasing the Mg content from 2-20% in an Al-Mg alloy, the corrosion current density increases in a saline environment.

However, there have been few studies on the effects of element addition on the electrochemical behaviors incorporating microstructure characterization in 5xxx Al alloy. In this study, anodizing and electrochemical behaviors of 5xxx Al alloy with different Mg and Cr addition were investigated. The effect of chloride concentration on the corrosion of 5xxx alloy will also be

considered. Potentiodynamic polarization curves and electrochemical impedance spectroscopy were utilized to investigate the effects on the corrosion and electrochemical behavior. The effect of CIE( $L^*$ ,  $a^*$ ,  $b^*$ ) color space of anodic oxide films was measured by spectrophotometer. The microstructure characterization was conducted by scanning electron microscopy and transmission electron microscopy (TEM).

## 2. EXPERIMENTAL METHOD

### 2.1 Materials

Chemical compositions of custom made 5xxx Al alloy sheets were given in Table 1, where it could be seen that Mg and Cr contents are varied respectively. The alloy sheets were prepared by casting from commercial purity materials. Alloying elements contents were analyzed by using inductively coupled plasma atomic emission spectroscopy (ICP-AES).

### 2.2 Anodizing treatment

Before anodizing, all specimens were degreased in acetone and rinsed in deionized water. Degreasing was followed by etching in 10 wt % NaOH for 5 mins at 45°C. After etching, any smut present on the specimens was removed by immersion in 30 vol % HNO<sub>3</sub> for 3 mins at room temperature. Anodizing was undertaken on custom made 5xxx Al alloy specimens in 20wt% sulfuric acid at 20°C. Furthermore, the anodized samples were sealed in hot water at 95°C for 900 s. After sealing, the thickness of the anodic oxide film was measured by eddy current using a calibrated Fischer Dualscope FMP 20. In addition, the CIE( $L^*$ ,  $a^*$ ,  $b^*$ ) color space of the anodic oxide film was measured by Konica Minolta CM-2600d spectrophotometer.

### 2.3 Electrochemical characterization

Corrosion tests were performed in H<sub>2</sub>SO<sub>4</sub> or NaCl aqueous solution at 25°C prepared with analytical reagents. Electrochemical techniques employed included linear potentiodynamic polarization curves, and electrochemical impedance spectroscopy measurements. The electrochemical tests were performed using a Princeton Applied Research VersaSTAT3 potentiostat, along with

a three electrode glass cell incorporating a Pt counter electrode and a silver chloride electrode (Ag/AgCl) as a reference electrode. Prior to testing, all the specimens were ground to 2000 grit SiC paper finish, and all the electrochemical tests were initiated after 30 min at the open circuit potential (OCP) of each specimen. Polarization curves were recorded at a constant sweep rate of 1 mV/s at the interval from -200 to +600 mV with respect to the open circuit potential,  $E_{\text{corr}}$ . Electrochemical impedance spectroscopy tests were carried out at  $E_{\text{corr}}$  by using a signal with an amplitude of 10 mV and a frequency interval of 0.05 Hz-100 kHz.

### 2.4 Microstructure observation

The samples of custom made 5xxx Al alloy were examined using a JEOL JSM-6510 SEM incorporating with energy dispersive X-ray spectroscopy (EDS) before and after potentiodynamic polarization tests. Microstructure of anodic oxide films was observed by a JEOL-2010 transmission electron microscopy operated at 200kV.

## 3. RESULTS AND DISCUSSION

### 3.1 Influence of Mg and Cr on the anodic oxide film

The anodizing treatment was carried out in a sulfuric acid electrolyte at a constant voltage of 20 V. The influence of Mg and Cr addition on the color of anodic oxide film is shown in Fig.1. In the defined CIE( $L^*$ ,  $a^*$ ,  $b^*$ ) color space measured by spectrophotometer, the lightness value,  $L^*$ , represents the darkest black at  $L^*=0$ , and the brightest white at  $L^*=100$ . In addition,  $b^*$  axis represents the blue–yellow component, with blue in the negative direction and yellow in the positive direction.

Fig.1(a) shows the effects of Cr addition on the color of anodic oxide film. At the same thickness, the  $b^*$  value increases with increasing of Cr content. The reason may be that Cr content changes the structure and density of the anodic oxide layer during the anodizing treatment, thereby increasing the intensity of reflected yellow light, so that the oxide film exhibits dark yellow color. Fig.1(b) shows the effects of Mg addition on the color of anodic oxide film. In contrast, the  $b^*$  value

**Table 1** The chemical compositions of custom made 5xxx Al alloy under study (wt%).

Alloy	Mg	Cr	Si	Fe	Mn	Al
Al-2wt%Mg	2.3	0.0	0.06	0.15	0.01	Bal.
Al-4wt%Mg	4.1	0.0	0.07	0.13	0.01	Bal.
Al-Mg-(Cr)	2.3	0.2	0.08	0.25	0.03	Bal.
Al-Mg	2.3	0.0	0.08	0.24	0.03	Bal.

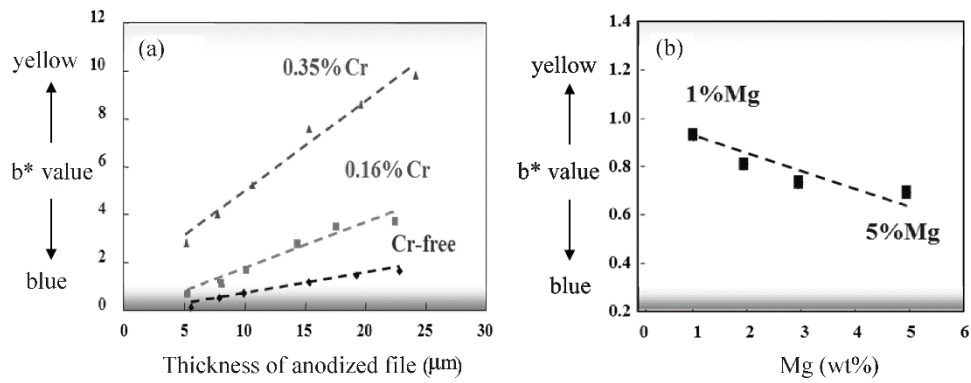


**Fig.1.** Influence of (a) Cr and (b) Mg content on b\*-value of anodic oxidized 5xxx alloy.

decreases with increasing of Mg content. The color of anodic oxide film shifts to blue with Mg addition.

Fig.2 shows the microstructure of the porous anodic oxide film observed by TEM. It can be seen that the space of columnar structure of the porous anodic oxide films changes to be narrower with Cr addition, therefore, the optical path in the anodic oxide films is different and the color of the oxide film is also changed.

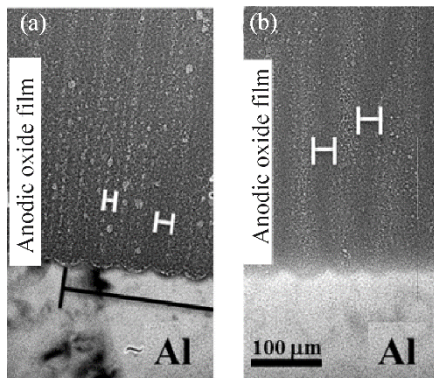


**Fig.2.** TEM observation of the porous anodic oxide film (a) Cr-free, (b) with Cr addition.

### 3.2 Microstructural characterization

In order to identify the intermetallic compounds present in the custom made 5xxx Al alloy, samples polished to mirror quality were studied by the SEM with EDS analysis. The results obtained indicate that intermetallic compounds such as those shown in Fig.3(a) can mainly be divided into two categories: white-grey Al-Fe-(Mn) and dark-colored Mg-Si particles. Fig.3(b) & (c) show the intensity of intermetallic particles are almost the same in the custom made 5xxx alloys with and without Cr addition. Cr addition has little effect on the microstructure of 5xxx Al alloy.

In contrast, the intensity of dark-colored Mg-Si particles is higher in the Al-4wt%Mg alloy. The intensity of Mg-Si particles increases with increasing Mg content. Hence, with Mg addition, the microstructure of 5xxx Al alloy is changed. Table 2<sup>(12)</sup> shows the corrosion potential of common intermetallic compounds in 5xxx Al alloy, it can be seen that Al-Fe-(Mn) has a higher corrosion potential than that of a Mg-Si particle, which indicates that intermetallic particles may affect the corrosion behavior of the Al alloy.

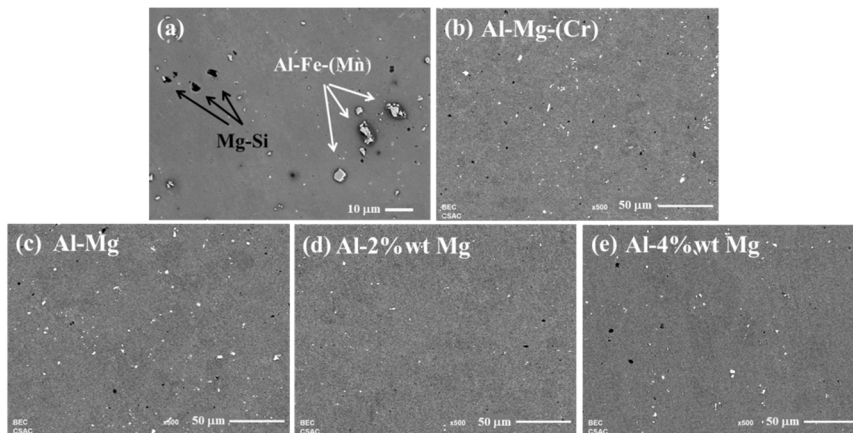


**Fig.3.** SEM observation of custom made 5xxx Al alloys under study.

### 3.3 Electrochemical behaviors

#### 3.3.1 Potentiodynamic polarization

The potentiodynamic polarization curve is a helpful tool in determining the instantaneous corrosion rate of a substrate. In a typical polarization curve, a lower corrosion current density ( $I_{\text{corr}}$ ) or a higher corrosion potential ( $E_{\text{corr}}$ ) corresponds to a lower corrosion rate and a better corrosion resistance<sup>(13)</sup>. The typical potentiodynamic polarization curves for the custom made 5xxx alloys are shown in Fig.4 which reveals the influence of Mg and Cr additions on the electrochemical characteristics. Fig.4(a) shows the polarization curves of Al-2wt%Mg and Al-4wt%Mg alloy in solution of 0.05M H<sub>2</sub>SO<sub>4</sub>. It can be observed that the corrosion potential of the Al-Mg alloy decreases with increasing Mg content, and the corrosion current density also increases with higher Mg-containing alloy ( $2.4 \times 10^{-5} > 1.6 \times 10^{-5}$  A/cm<sup>2</sup>). That indicates that with higher Mg-containing, Al-4wt%Mg is more susceptible to corrosion, and the corrosion rate is faster when it corrodes. It may also be associated with that Al-4wt%Mg alloy has more low corrosion potential Mg-Si particles (less noble), as shown in Fig.3(e).

Fig.4(b) shows the corrosion polarization curves of custom made 5xxx Al alloy with and without Cr addition

in a solution of 0.05M H<sub>2</sub>SO<sub>4</sub>. With Cr addition, the alloy has a higher corrosion potential and a lower corrosion current density ( $1.6 \times 10^{-5} < 1.8 \times 10^{-5}$  A/cm<sup>2</sup>), which means that 5xxx Al alloy has better corrosion resistance with the presence of Cr element. Based on the potentiodynamic polarization tests, it is harmful for corrosion resistance of 5xxx alloy with higher Mg content. On the contrary, Cr addition is a benefit for improving corrosion resistance.

#### 3.3.2 Electrochemical impedance spectroscopy

EIS data measured in sulfuric acid solution in Nyquist format is shown on Fig.5. The analytical software is used for the parameter fitting and the fitting circuit model is shown in Fig.6, where  $R_s$  represents the solution impedance and  $R_t$  represents the charge transfer resistance, the constant phase angle element CPE1 is the electrode double layer capacitance of the electrode surface; the obtained equivalent circuit component fitting parameters are shown in Table 3. Nyquist plots for all samples show a capacitive-like semicircle at high and intermediate frequency values which correspond to a charge transfer mechanism from the alloy to the environment to the double electrochemical layer. The diameter of the capacitive semicircle corresponds to the charge

**Table 2** Corrosion potential of intermetallic compounds in 5xxx Al alloy (ASTM G 69)<sup>(12)</sup>.

Intermetallic phases	Corrosion potential, V <sub>SCE</sub> (Ref. 12)
Al <sub>3</sub> Fe	-0.47
Al <sub>6</sub> (Fe, Mn)	-0.76
Al-3wt%Mg	-0.78
Al <sub>3</sub> Mg <sub>2</sub>	-1.15
Mg <sub>2</sub> Si	-1.19

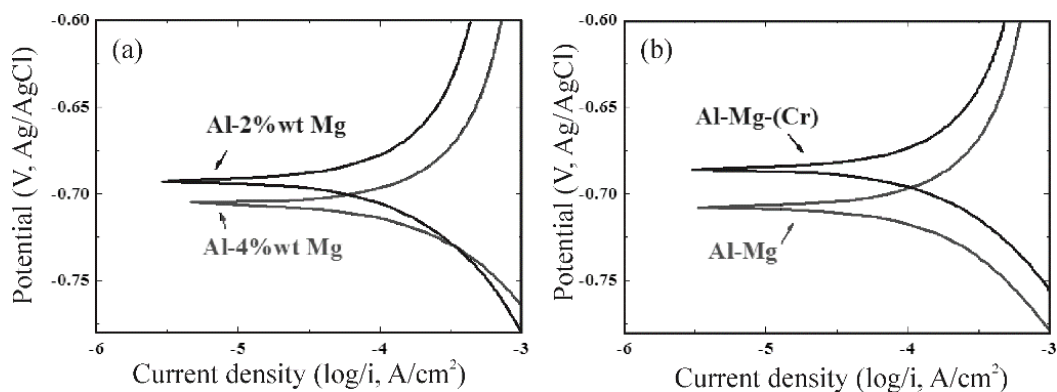


**Fig.4.** Potentiodynamic polarization curves for (a) Al-2wt%Mg & Al-4wt%Mg alloy, and (b) Al-Mg-(Cr) & Al-Mg alloy collected in 0.05M H<sub>2</sub>SO<sub>4</sub> solution.

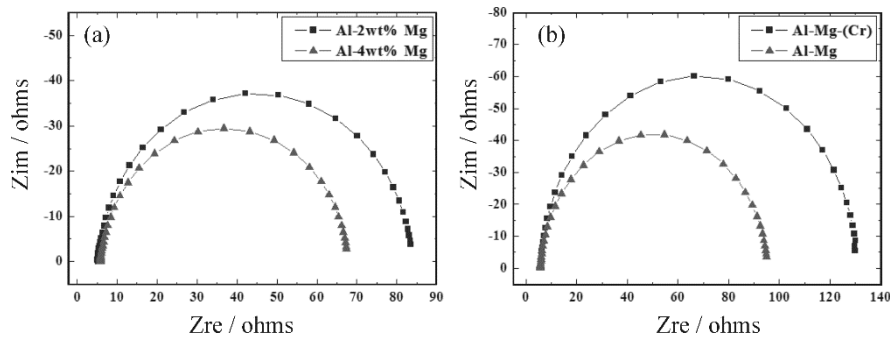


**Fig.5.** Effect of (a) Mg addition, and (b) Cr addition on the impedance response of 5xxx Al alloy in 0.05M H<sub>2</sub>SO<sub>4</sub> solution at OCP.

**Table 3** Optimum fit parameters for experiments in Fig.5.

Alloy	$R_s/\Omega\cdot\text{cm}^2$	$\text{CPE-T}/\text{F}\cdot\text{cm}^2$	$\text{CPE-P}/\text{F}\cdot\text{cm}^2$	$R_t/\Omega\cdot\text{cm}^2$
Al-2wt%Mg	5.1	$2.1\cdot 10^{-4}$	0.95	79.36
Al-4wt%Mg	5.8	$2.5\cdot 10^{-4}$	0.95	62.33
Al-Mg-Cr	5.8	$1.5\cdot 10^{-4}$	0.97	125.2
Al-Mg	5.7	$1.9\cdot 10^{-4}$	0.96	89.66

transfer resistance, and it is much bigger for custom 5xxx alloys with Al-2wt%Mg and Al-Mg-(Cr) alloys than that for Al-4wt%Mg and Al-Mg alloys, respectively. The Nyquist plot and fitting results indicate that Cr-containing alloy and lower Mg-containing alloy has a higher corrosion resistance than that of Al-Mg alloy without Cr addition and with higher Mg-content, just as illustrated by the polarization curves, Fig.4.



**Fig.6.** The equivalent circuit model used to fit.

### 3.4 Effect of chloride concentration on corrosion

Chloride is a common impurity element in aqueous solution, and causes metal corrosion easily. Fig.7 shows typical anodic polarization curves obtained with samples of 5xxx aluminum alloy exposed to NaCl solutions at different concentrations. The anodic behavior of samples during exposure to 0.1M up to 1M NaCl solutions are similar, each exhibiting pitting potential  $E_{\text{pit}}$  at the corrosion potential  $E_{\text{cor}}$ . The curves show that the increasing in the chloride concentration produces a decreasing in corrosion potential  $E_{\text{cor}}$  and an increasing in cathodic corrosion current density  $I_{\text{cathodic}}$  of the samples of custom made Al alloy. It indicates that an increase in the concentration of chloride will promote the corrosion

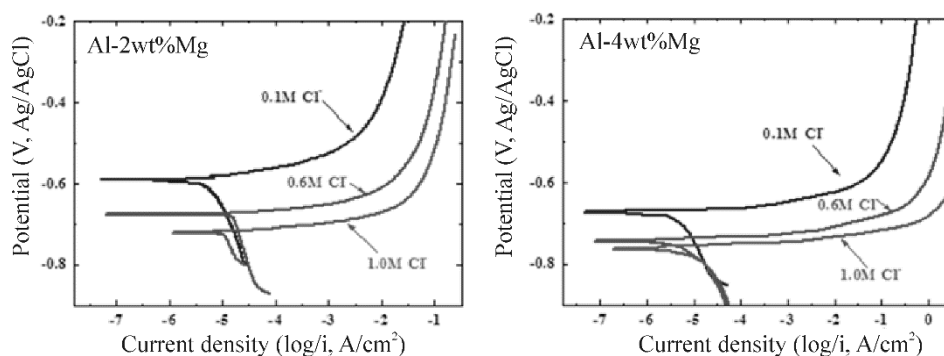


**Fig.7.** Potentiodynamic polarization curves for Al-2wt%Mg and Al-4wt%Mg alloy in NaCl solution with different chloride concentration.

reaction, making the aluminum alloy more susceptible to corrosion. On the basis of the polarization curve results, chloride is a strong factor causing corrosion. Hence, it is necessary to control the quality of aqueous solution or oil used during the Al sheet production process, in order to prevent corrosion defects caused by chloride.

### 3.5 Morphology of corrosion attack

Fig.8 shows the SEM micrographs of the corroded surfaces of the samples after the potentiodynamic polarization in 0.05M H<sub>2</sub>SO<sub>4</sub> or 0.6M NaCl solution. It can be seen that pitting occurs in all samples, where Al-Mg alloy with Cr addition has shallow etched pores and the Al-4wt%Mg alloy exhibits the deepest etched pores. As for the chloride-containing environment, many small holes (pointed out by the arrow) can be observed on the surface beside the main pitting holes. Those are supposed to be the initial stages of pitting corrosion but not yet growing, that is, the presence of chloride will make the aluminum surface corrode more vigorously and freely, and this microscopic observation is consistent with the electrochemical analysis described previously.

In order to investigate the corrosion evolution of 5xxx Al alloy, the potentiodynamic polarization test was cutoff at different potentials which was utilized to control the surface corrosion stages. Fig.9(a) shows the interface of white-grey Al-Fe intermetallic particles with higher corrosion potential (more noble) and relative

lower corrosion potential Al matrix (less noble). It can be observed that corrosion starts from Al matrix and continues to the dissolution of Al matrix, which is served as a local anode. Finally, the etching hole is enlarged gradually and only the high corrosion potential Al-Fe particles, serving as local cathode, are left. Fig.9(b) shows the interface of dark-colored Mg-Si intermetallic particles and Al matrix. Oppositely, the Mg-Si particle with lower corrosion potential is served as a local anode and itself undergoes dissolution (independent of the matrix). The damage accumulation takes the form of incongruent dissolution. According to the above results, it is evident that the initial corrosion takes place from the interface with the corrosion potential drop.

## 4. CONCLUSIONS

Electrochemical measurements combined with microstructural characterization of 5xxx Al alloy with different Mg and Cr addition were studied in this study. The results showed:

- (1) The color of anodic oxide film were influenced by Mg and Cr addition. The  $b^*$  value of anodic oxide film decreased with Mg addition and the color shifted in the blue direction. With Cr addition, the space of columnar structure of the porous anodic oxide films was narrower and the  $b^*$  value also increased, so the color shifted to be yellow.
- (2) Through the potentiodynamic polarization curve and EIS tests, Cr was a protective role when added, and

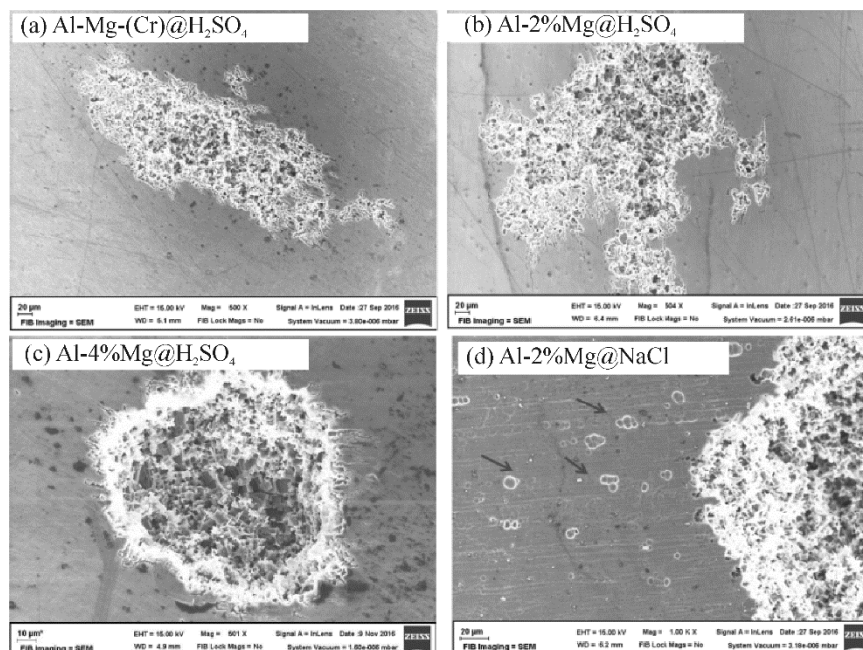
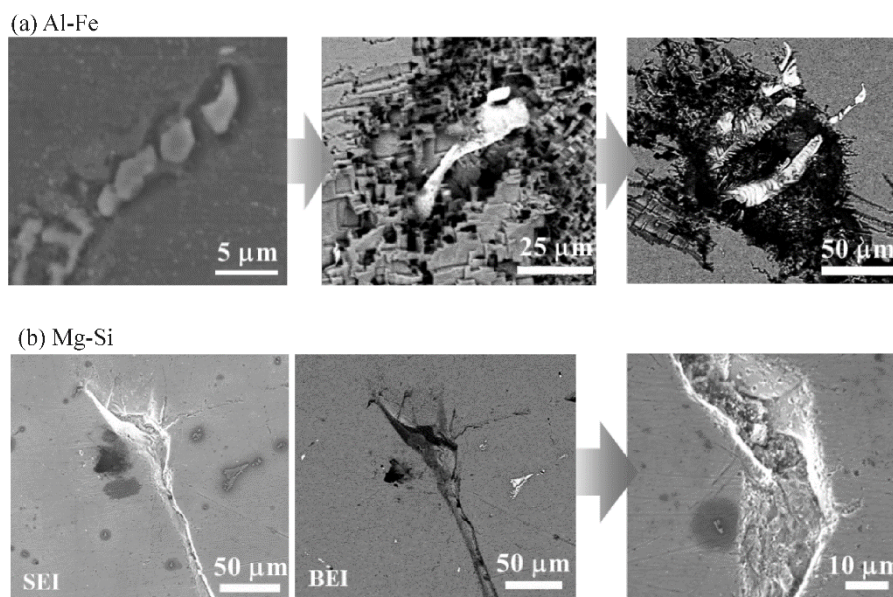


Fig.8. SEM micrographs of corroded surface of samples after polarization tests in H<sub>2</sub>SO<sub>4</sub> or NaCl solution.



**Fig.9.** The micrographs of interface between matrix and (a) higher potential Al-Fe intermetallic particles, (b) lower potential Mg-Si intermetallic particles during the corrosion process, show initial corrosion attack takes place on interface with potential drop.

made the corrosion potential and impedance rise which improved the corrosion resistance of 5xxx Al alloy. In contrast, the 5xxx Al alloy was more susceptible to corrosion with Mg addition due to the decrease of corrosion potential and impedance, and an increase of corrosion current density.

- (3) 5xxx Al alloy was susceptible to pitting corrosion in chloride solution and an increase in the chloride concentration shifted the corrosion potentials to more active values. During the corrosion process, the initial corrosion attack took place on the interface with a potential drop, such as interface between Mg-Si or Al-Fe particles. Mg-Si particles were anodic as compared to the surrounding matrix and experienced dissolution itself. In contrast, Al-Fe particles were cathodic to the surrounding matrix and corrosion starts from Al matrix.

## REFERENCES

1. A.V. Sameljuk, O.D. Neikov, A.V. Krajinikov, Y.V. Milman, G.E. Thompson, and X. Zhou, *Corros. Sci.*, 2007, vol. 49, pp. 276-286.
2. S.M. Moon, M. Sakairi, and H. Takahashi, *J. Electrochem. Soc.*, 2004, vol. 151, pp. 399-405.
3. K. Shimizu, G.M. Brown, H. Habazaki, K. Kobayashi, P. Skeldon, G.E. Thompson, and G.C. Wood, *Corrosion Science*, 2000, vol. 42, pp. 831-840.
4. J. De Laet, X. Zhou, P. Skeldon, G.E. Thompson, G.C. Wood, H. Habazaki, K. Takahiro, S. Yamaguchi, and K. Shimizu, *Corrosion Science*, 1999, vol. 41, pp. 213-227.
5. M. Jariyaboon, P. Moller, R.E. Dunin-Borkowski, and R. Ambat, *Anti-Corrosion, Methods and Materials*, 2011, vol. 58, pp. 173-178.
6. L.E. Fratila-Apachitei, H. Terryn, P. Skeldon, G.E. Thompson, J. Duszczyk, and L. Katgerman, *Electrochimica Acta*, 2004, vol. 49, pp. 1127-1140.
7. T. Tanaka, T. Saito, and H. Kawase, *Light Metal*, 1972, vol. 22, pp. 39-46.
8. T. Ohnishi, Y. Nakatani, and K. Shimizu, *Light Metal*, vol. 23, pp. 58-65.
9. Y. Ishikawa, *Light Metal*, 1967, vol. 17, pp. 20-28.
10. L. Vrsalovic, M. Kliskic, and S. Gudic, *Int. J. Electrochem. Sci.*, 2009, vol. 4, pp. 1568-1582.
11. K.R. Baldwin, R.I. Bates, R.D. Arnell, and C.J.E. Smith, *Corros. Sci.*, 1996, vol. 38, pp. 155-170.
12. Christian Vargel: *Corrosion of Aluminium*, Elsevier Ltd., Oxford, UK, 2004, pp. 96-101.
13. X. Li, X. Nie, L. Wang, and D.O. Northwood, *Surf. Coat. Tech.*, 2005, vol. 200, pp. 1994-2000. □